

## Synthesis of Nickel Hierarchical Microstructures by a Simple Hydrothermal Route

Guo-Bin Cheng,<sup>1,\*</sup> Gui-Chen Wei,<sup>2</sup> Cheng-Jun Hao,<sup>1</sup> and Song-Tian Li<sup>1</sup>

<sup>1</sup>School of Chemistry and Chemical Engineering, Pingdingshan University,  
Pingdingshan, 467000, Henan, P. R. China

<sup>2</sup>Xuchang Environmental Protecting Research Institute, Xuchang, 461000, Henan, P. R. China

Nickel hierarchical microstructures have been synthesized from the reduction of nickel hydrazine complexes by a simple hydrothermal method. The samples were characterized by X-ray diffraction (XRD), scanning electron microscopy (SEM), transmission electron microscopy (TEM), and superconducting quantum interference device (SQUID). The results indicated that the Ni hierarchical microstructures are face-centered cubic phase with a size of 2-3  $\mu\text{m}$  for a single hierarchical microstructure while some thick petals with a length in the range of 0.5-1.5  $\mu\text{m}$  extrude around the surface. The value of coercivity reached 121 Oe at room temperature, which is vastly superior to that of bulk nickel. Parallel experiments showed that the hydrothermal reaction time and the presence of surfactant cetyltrimethylammonium bromide (CTAB) played important roles in the formation of such hierarchical morphology.

**Keywords:** hydrothermal synthesis, nanostructures, nickel

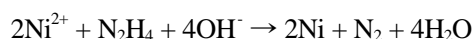
### 1. INTRODUCTION

During the past few decades, nanomaterials have attracted considerable attention due to both their unique properties of being quite different from those of bulk materials and their potential applications in many areas such as sensors, solar cells, and catalysis.<sup>[1-5]</sup> To control the morphology of inorganic materials at the micro- and nano-scale level is one of the hot issues for material chemists because the intrinsic properties of nanomaterials are closely related to their morphology, size, and crystallinity.<sup>[6,7]</sup>

As an important anisotropic ferromagnetic metal, nickel micro- and nanostructures have drawn great interest because of their potential technological applications such as magnetic recording media, chemical catalysts, and conducting materials.<sup>[8-10]</sup> Up to now, many kinds of nickel micro- and nanostructures have been synthesized via various approaches including hydrothermal reduction, electrodeposition, and non-aqueous Sol-Gel method.<sup>[11-14]</sup> For example, Qian and co-workers fabricated ferromagnetic Ni nanobelts by reduction of a Ni tartrate with the assistance of sodium dodecylbenzenesulfonate (SDBS).<sup>[15]</sup> Xu and co-workers prepared hollow Ni sub-micrometer spheres, nanometer-sized Ni hollow spheres, and highly-ordered Ni nanotube arrays and have studied their magnetic properties, respectively.<sup>[16-18]</sup>

Other special morphologies such as triangular and hexagonal Ni nanosheets, flowerlike Ni nanostructure and microstructures, Ni nanochains, and sea urchin-like Ni nanocrystals were also successfully achieved.<sup>[19-29]</sup> However, to the best of our knowledge, it is still challenging to fabricate nickel hierarchical microstructures under mild conditions.

In this paper, we put forward a facile hydrothermal method to synthesize Ni hierarchical microstructures using aqueous hydrazine as a reducing agent and cetyltrimethylammonium bromide (CTAB) as a surfactant. The morphology of the final product can be easily controlled by adjusting the hydrothermal reaction time. The presence of CTAB is also critical to producing such Ni microstructures. The reduction reaction can be expressed as the following:



### 2. EXPERIMENT

All analytical chemical reagents were purchased from Shanghai Chemical Reagents Company and used without further purification. In a typical synthesis, 4 mmol  $\text{NiCl}_2 \cdot 6\text{H}_2\text{O}$  was dissolved into 20 mL deionized water, then 10 mL 5 mol/L NaOH solution and 4 mmol CTAB were added to the above  $\text{Ni}^{2+}$  solution under vigorous stirring for 30 min. This was followed by the addition of 10 mL hydrazine hydrate ( $\text{N}_2\text{H}_4 \cdot \text{H}_2\text{O}$ , 80 wt.%) and after 10 min more continuous stirring, the mixed solution was loaded into a 50

\*Corresponding author: cheng2002\_hn@163.com

mL Teflon-lined stainless-steel autoclave, sealed, and kept at 120 for 36 h. The resultant black precipitate was filtered, and then rinsed with distilled water and absolute ethanol several times. The final product was dried in a vacuum oven at 50°C for 6 h.

The phase of the as-synthesized samples was characterized by x-ray powder diffraction (XRD) using a Shimadzu XRD-6000 diffractometer with  $\text{CuK}\alpha$  ( $\lambda = 1.54060 \text{ \AA}$ ) radiation (40 kV, 30 mA). The scanning rate was  $4^\circ/\text{min}$  and  $2\theta$  ranges from  $40^\circ$  to  $100^\circ$  at room temperature. The structures and morphologies of the products were examined by scanning electron microscope (SEM, JEOL JSM-5600LV) and transmission electron microscope (TEM, Philips Tecnai G<sup>2</sup> 20) with an accelerating voltage of 200 kV. The magnetic properties were investigated by a SQUID magnetometer (MPMS XL-7T, Quantum Design) with an applied field up to 6 kOe.

### 3. RESULTS AND DISCUSSION

Figure 1 shows the typical XRD patterns of the as-synthesized nickel samples: all the diffraction peaks of (111), (200), (220), (311), and (222) match well with the Ni face-centered cubic (fcc) structure (JCPDS card No. 04-0850) and the sample prepared here is well crystallized. No impurities such as NiO or  $\text{Ni}(\text{OH})_2$  were detected. This indicated that a pure metallic Ni product can be obtained through the current synthetic approach.

The morphologies and structures of the samples were further examined by scanning electron microscope (SEM) and transmission electron microscopy (TEM). From the panoramic SEM images in Fig. 2(a), nickel hierarchical microstructures can be clearly observed and the products exhibit a flowerlike shape, to some extent. Detailed investigation about such morphology is displayed with high-magnification SEM images in Figs. 2(b) and (c). Some thick petals

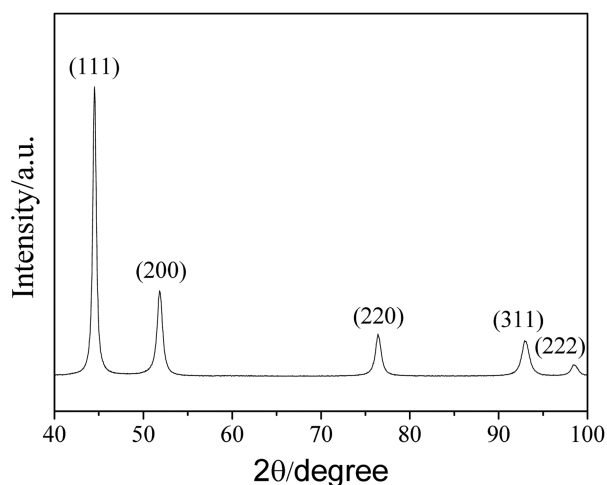


**Fig. 1.** XRD patterns of the as-prepared hierarchical nickel microstructures.

with a length in the range of  $0.5 \mu\text{m}$  to  $1.5 \mu\text{m}$  are observed and these petals integrated to form larger hierarchical microstructures with a size of about  $2 \mu\text{m}$  to  $3 \mu\text{m}$ . From the TEM image shown in Fig. 3(a), there are several nickel hierarchical microstructures that are connected. Rod-like and flake-like petals with a length of about  $0.5 \mu\text{m}$  to  $1 \mu\text{m}$  extrude around the surface of such Ni hierarchical microstructures and the results are consistent with what was observed from the SEM images. The corresponding selected area electron diffraction (SAED) shown in Fig. 3(b) indicates that such nickel hierarchical microstructures are polycrystalline.

Several parallel experiments were carried out to explore the growth process for such Ni microstructures. The results showed that the hydrothermal reaction time and the presence of CTAB are two important factors to the formation of such morphology. Some particles with small nanothorns on the surface were generated when the reaction processed in 8 hours while other parameters remained constant. The nanothorns would grow larger as the reaction time increased, until the final hierarchical microstructures were produced. The evolution process of the morphology is obvious from the SEM images in Figs. 2(d) and (e). On the basis of the SEM observations, the formation of hierarchical nickel microstructures is a typical Ostwald ripening process.  $\text{NiCl}_2$  can be transformed into  $\text{Ni}(\text{NH}_3)_6\text{Cl}_2$  in a hydrazine hydrate

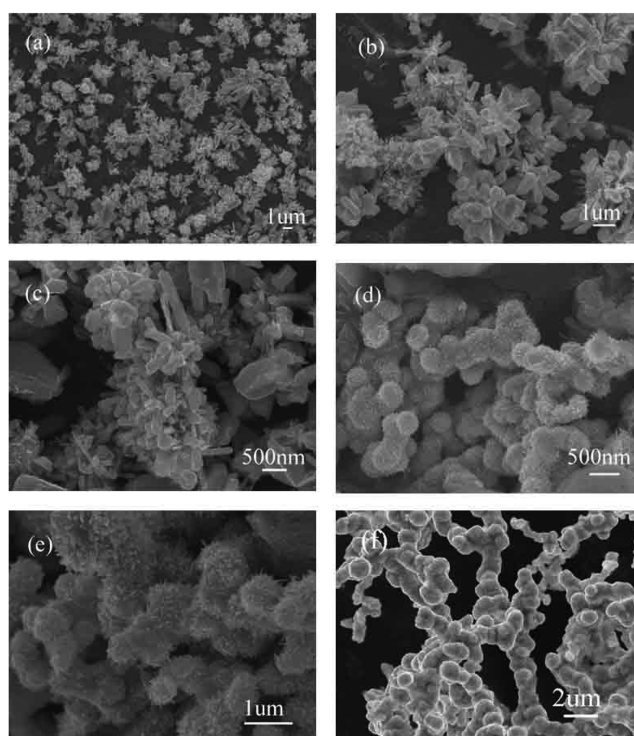


**Fig. 2.** SEM images of the resultant nickel samples. (a-c) images with different magnifications of Ni hierarchical microstructures prepared at 120 for 36 h; samples synthesized at 120 for (d) 8 h and (e) 16 h; (f) products obtained at 120 for 16 h without CTAB.

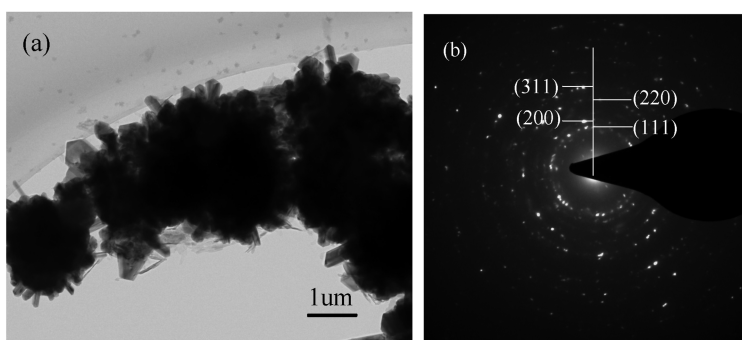


**Fig. 3.** TEM image of Ni hierarchical microstructures (a) obtained at 120 for 36 h, and (b) the SAED pattern.

aqueous solution, then  $\text{Ni}(\text{NH}_3)_6\text{Cl}_2$  is reduced by hydrazine hydrate resulting in the generation of Ni atoms at the initial stage. With the reaction progressing, the existing Ni nanoparticles could serve as the seeds for the further growth of larger particles at the expense of the small nanoparticles through Ostwald ripening until hierarchical microstructures finally formed.

The existence of a surfactant CTAB is also important in the current synthetic system. Generally, the surfactant is considered to kinetically control the growth rates of different crystallographic facets of nickel micro- and nanostructures through preferentially adsorbing and desorbing these facets. If the same method and synthetic parameters are employed in the absence of CTAB, only nickel micro-particles with a diameter of about 1  $\mu\text{m}$  can be obtained and the particles aggregate together. Fig. 2(f) shows the SEM image of the as-prepared nickel samples obtained at 120°C for 16 h without CTAB. The detailed mechanism for the formation of such morphology is still unclear at present and related research is under way.

It is believed that the magnetic properties of nanomaterials have a close relationship with their morphologies, crystallinity, magnetization direction, and so on. The hysteresis loop (Fig. 4) of the nickel hierarchical microstructures measured

at room temperature displays a ferromagnetic behavior with saturation magnetization ( $M_s$ ), remanent magnetization ( $M_r$ ), and coercivity ( $H_c$ ) values of about 52 emu/g, 9 emu/g, and 121 Oe, respectively. Compared to the  $H_c$  value of bulk Ni (ca. 0.7 Oe) and that of hollow nickel sub-micrometer spheres (ca. 32.3 Oe),<sup>[16]</sup> nickel hierarchical microstructures exhibit much enhanced coercivity, which may be a result of these special hierarchical structures.

#### 4. CONCLUSIONS

Nickel hierarchical microstructures with a size of 2-3  $\mu\text{m}$  were synthesized at 120°C for 36 h via a hydrothermal approach and hydrazine hydrate was used as a reducing reagent. The investigation of the evolution process of such morphology demonstrated that the hydrothermal reaction time and the existence of CTAB were crucial factors to generate the resultant nickel structures. The nickel hierarchical microstructures obtained through our current synthetic route showed much enhanced coercivity values compared to that of bulk nickel, probably due to their special hierarchical structures.

#### REFERENCES

1. S. Ghosh, A. K. Sood, and N. Kumar, *Science* **299**, 1042 (2003).
2. Y. G. Sun and H. H. Wang, *Adv. Mater.* **19**, 2818 (2007).
3. W. U. Huynh, J. J. Dittmer, and A. P. Alivisatos, *Science* **295**, 2425 (2002).
4. P. Gao, M. L. Zhang, H. W. Hou, and Q. P. Xiao, *Mater. Res. Bull.* **43**, 531 (2008).
5. S. W. Cao, Y. J. Zhu, M. Y. Ma, L. Li, and L. Zhang, *J. Phys. Chem. C* **112**, 1851 (2008).
6. Y. G. Sun and Y. N. Xia, *Science* **298**, 2176 (2002).
7. K. Nagaveni, A. Gayen, G. N. Subbanna, and M. S. Hegde, *J. Mater. Chem.* **12**, 3147 (2002).
8. H. L. Niu, Q. W. Chen, M. Ning, Y. S. Jia, and X. J. Wang, *J. Phys. Chem. B* **108**, 3996 (2004).
9. S. Pignard, G. Goglio, A. Radulescu, L. Piraux, S. Dubois, A. Declémy, and J. L. Duvail, *J. Appl. Phys.* **87**, 824

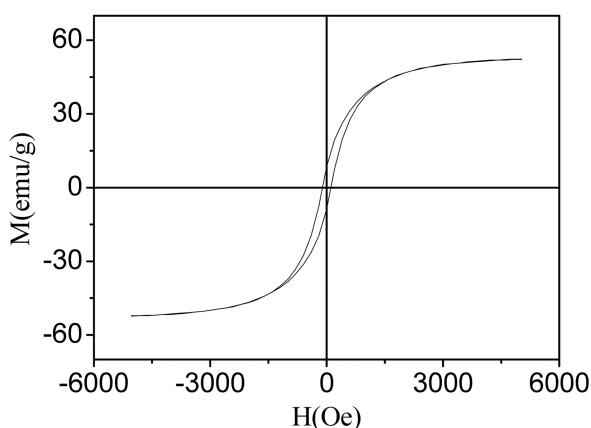


**Fig. 4.** Hysteresis loop for hierarchical nickel microstructures at room temperature.

- (2000).
10. D. H. Chen and C. H. Hsieh, *J. Mater. Chem.* **12**, 2412 (2002).
  11. Y. D. Li, L. Q. Li, H. W. Liao, and H. R. Wang, *J. Mater. Chem.* **9**, 2675 (1999).
  12. C. L. Jiang, G. F. Zou, W. Q. Zhang, W. C. Yu, and Y. T. Qian, *Mater. Lett.* **60**, 2319 (2006).
  13. J.C. Bao, C.Y. Tie, Z. Xu, Q.F. Zhou, D. Shen, and Q. Ma, *Adv. Mater.* **13**, 1631 (2001).
  14. F. L. Jia, L. Z. Zhang, X. Y. Shang, and Y. Yang, *Adv. Mater.* **20**, 1050 (2008).
  15. Z. P. Liu, S. Li, Y. Yang, S. Peng, Z. K. Hu, and Y. T. Qian, *Adv. Mater.* **15**, 1946 (2003).
  16. J. C. Bao, Y. Y. Liang, Z. Xu, and L. Si, *Adv. Mater.* **15**, 1832 (2003).
  17. Q. Liu, H. J. Liu, M. Han, J. M. Zhu, Y. Y. Liang, Z. Xu, and Y. Song, *Adv. Mater.* **17**, 1995 (2005).
  18. F. F. Tao, M. Y. Guan, Y. Jiang, J. M. Zhu, Z. Xu, and Z. L. Xue, *Adv. Mater.* **18**, 2161 (2006).
  19. D. G. Li, X. M. Ni, H. G. Zheng, and B. H. Qi, *Chem. Lett.* **37**, 148 (2008).
  20. Y. H. Leng, Y. T. Wang, X. G. Li, T. Liu, and S. Takahashi, *Nanotechnology* **17**, 4834 (2006).
  21. X. M. Ni, Q. B. Zhao, J. Cheng, H. G. Zheng, B. B. Li, and D. G. Zhang, *Chem. Lett.* **34**, 1408 (2005).
  22. X. M. Ni, Q. B. Zhao, H. G. Zheng, B. B. Li, J. M. Song, D. G. Zhang, and X. J. Zhang, *Eur. J. Inorg. Chem.* **23**, 4788 (2005).
  23. X. M. Ni, Y. F. Zhang, J. M. Song, and H. G. Zheng, *J. Cryst. Growth* **299**, 365 (2007).
  24. C. M. Liu, L. Guo, R. M. Wang, Y. Deng, H. B. Xu, and S. H. Yang, *Chem. Commun.* 2726 (2004).
  25. X. H. Liu, X. D. Liang, N. Zhang, G. Z. Qiu, and R. Yi, *Mater. Sci. Eng. B* **132**, 272 (2006).
  26. Y. Wang, Q. S. Zhu, and H. G. Zhang, *Mater. Res. Bull.* **42**, 1450 (2007).
  27. X. M. Ni, X. B. Su, Z. P. Yang, and H. G. Zheng, *J. Cryst. Growth* **252**, 612 (2003).
  28. Y. D. Deng, X. Liu, B. Shen, L. Liu, and W. B. Hu, *J. Magn. Magn. Mater.* **303**, 181 (2006).
  29. Y. Wang, Q. S. Zhu, and H. G. Zhang, *J. Mater. Chem.* **16**, 1212 (2006).